A New Analysis of the Normal Modes of a Large English Church Bell

Hamish Whyte (1), Robert Perrin (1) and Benjamin Halkon (1,2)

(1) School of Mechanical and Mechatronic Engineering, Faculty of Engineering and IT,
(2) Centre for Audio, Acoustics and Vibration, Faculty of Engineering and IT,
University of Technology Sydney, Ultimo, NSW 2076, Australia

Abstract – The present paper reports on the use of a modern "state-of-the-art" FE package to re-examine the normal modes of a large (214 kg) English church bell which first appeared in 1983. ABAQUS produced results in close agreement with experiment but, with its enhanced visualisation and post-processing capabilities, a more complete understanding of mode shapes that have previously been difficult to analyse, became possible. The ability to include superimposed deformation vectors in the visualisation of modes enabled them to be classified into three categories: those with predominantly (1) radial, (2) longitudinal and (3) tangential deformations, respectively. Resolving mode shape deformations into these directions, has allowed quantitative confirmation of the classifications. Relationships between the ratios of the deformation components and the symmetry properties of the modes are presented. The results are largely in line with expectations, including those derived from studies of the vibrations of cylinders and from group representation theory.

1 INTRODUCTION

The vibration and acoustic properties of axisymmetric structures are a topic of interest and importance in science and engineering. Vibration of axisymmetric structures has been investigated in many applications including in cylinders (Leissa, 1973), bells (Perrin et al.,1973, Perrin et al.,1983), cymbals (Perrin et al., 2008) and gongs (Perrin et al., 2014). A review for axisymmetric musical structures has been given by Rossing (1984). The English church bell is one such structure. Perrin et al. (1983) performed the most detailed modal analysis of the modern English church bell to date, with experimental results showing modes up to 9.3 kHz. Reasonable agreement was found with finite element analysis results from PAFEC (Program for Automated Finite Element Calculations). No similar research between this initial work and the current study is known to the authors.

Early investigations tended to concentrate on the first five "partials" of the bell, because of their musical significance (Rossing & Perrin, 1987). The term partial is used by campanologists and bell founders to describe the tonal components that make up the combined sound of the bell. Partials can either be singlet or degenerate doublet modes. Bell founders tune the musical modes to frequencies in the approximate ratios of 1: 2: 2.4: 3: 4 for a harmonious sound. Except for the work of Perrin et al. (1983), there has been less interest in the higher frequency "non-musical" modes. Beyond axisymmetric musical instruments, these methods have possible industrial applications involving cylinders, discs, rings and cones.

Group theory is a mathematical approach that allows the classification of modes into symmetry types and is well-used in vibration analysis in molecular chemistry (Wolbarst, 1977). The information is purely qualitative but enables prediction of degeneracy structures (Perrin & Charnley, 1973) (Charnley & Perrin, 1975). The standard bell is (approximately) axisymmetric so its symmetries are described (using cylindrical polar coordinates) by the well-known group $C_{\infty v}$ (Perrin & Charnley, 1973). The properties of this group show that the normal modes of the bell must be of the form $\sin(m\theta)$ or $\cos(m\theta)$ where m=0,1, etc.. The character table of the group shows that each mode is either a singlet (m=0) or a degenerate doublet (m>0). Thus, the normal modes have nodal patterns consisting of m equally spaced diameters across the top of the bell and n circles parallel to the rim (Perrin & Charnley, 1973).

In previous studies of the bell, it was concluded that deformations in musically significant modes are dominated radially and are primarily located around the rim of the bell (Perrin et al., 1983). Observations were also made of the presence of tangentially dominated torsional modes with m=0. The difficulty of experimentally identifying tangentially and longitudinally dominated modes, prevented observation of the full set of modes. Group theory predictions, together with knowledge of the modes of rings and cylinders, suggest that the bell should exhibit modes in three families: radially, tangentially and longitudinally dominant. The full extent of these modes, such as m>0 tangential modes, have been largely unobserved until now.

The experimental data obtained by Perrin et al. 1983 allow the normal modes of the Taylor bell to be re-studied using the ABAQUS 2023 finite element (FE) analysis package. The results can also be compared with earlier PAFEC counterparts. ABAQUS improved visualisation capability has allowed quantitative classification of the modes of the bell.

2 FINITE ELEMENT ANALYSIS

2.1 Pre-Processing

The earlier analysis of the Taylor Bell by Perrin et al. (1983) has provided a series of accurate datapoints taken across a cross-section of the bell, which were used as the basis for the original PAFEC computations. The data points were obtained in that study by experimentally measuring the bell, now located at Taylor's Bell Foundry in the UK. These data points have been imported into ABAQUS with splines constructed to achieve a relatively smooth surface profile. This profile was revolved to create the 3D geometry used in the FE analyses. The same material properties of the Bell Metal (E = 103 GPa, ρ = 8.85e-6 kg/mm^3, ν = 0.38) used in the PAFEC analysis were applied in the simulations. The overall bell height is 566 mm with a rim diameter of 702 mm. The resulting mass was 217 kg. Free-free boundary conditions were specified with a linear perturbation step to extract all frequencies over the range to 9 kHz. The meshed geometry, using quadratic tetrahedral C3D10 elements, of the bell is shown below in Figure 1.

2.2 Analysis/Solving

Frequency results and shapes were compared those from the original experimental and PAFEC modal frequencies (Perrin et al., 1983) as shown in Table 1 for a subset of the musical modes. It was concluded that the results of the simulation were acceptable, with the ABAQUS simulations exhibiting even better agreement with the experimental results than did those from PAFEC. It is noted that the PAFEC predictions always underestimate the resonant frequencies while the ABAQUS counterparts are sometimes higher and sometimes lower. It is believed that the closer agreement of the ABAQUS results can at least be partially attributed to the better agreement between the ABAQUS geometry more and that of the real bell. The ABAQUS geometry has more fidelity that that which was defined in PAFEC. Over the 9 kHz range, 261 modes were detected.

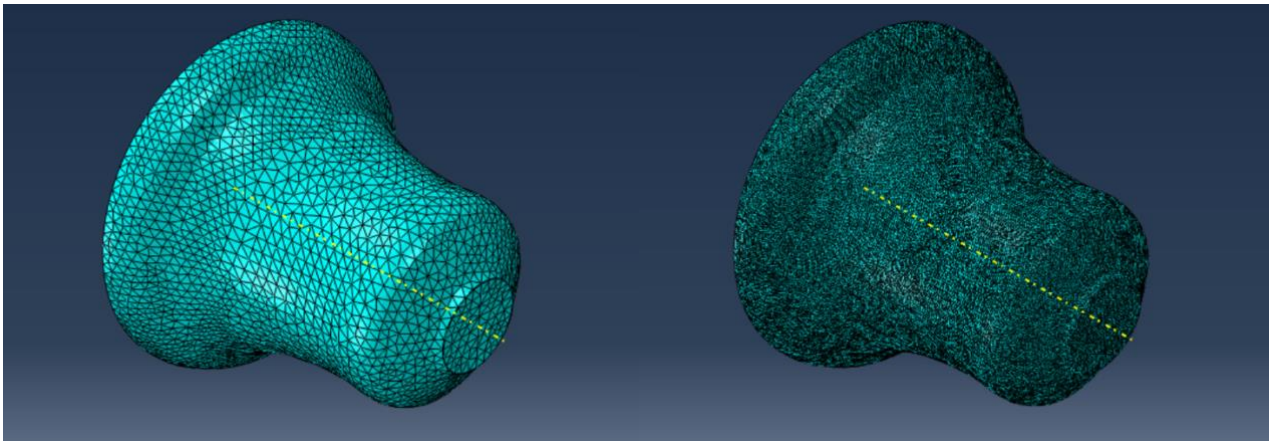

Figure 1 – Coarse mesh (left), seed size 20 and fine mesh (right), seed size 5; element type: C3D10

Table 1 – Comparison of musical mode set frequencies using m nomenclature

Musical name	m,n	Experimental frequency (Hz)	PAFEC frequency (Hz)	Difference PAFEC:Experiment (%)	ABAQUS frequency (Hz)	Difference ABAQUS:Experiment (%)
Hum	2,0	293	268	8.5	294	-0.3
Fundamental[$]	2,1	586	568	3.1	579	1.2
Tierce	3,1*	693	677	2.3	693	0.0
Quint	3,1	883	881	0.2	884	-0.1
Nominal	4,1*	1172	1166	0.5	1170	0.2
Superquint[#]	5,1*	1764	1762	0.1	1757	0.4

[$]Name generally used by British bell founders for this, not the lowest frequency, mode
[#]Can often be included in “musical modes”

2.3 Post-Processing

Using the post-processing capabilities of ABAQUS, qualitative analysis was conducted of the mode shapes. It was observed that the mode shapes could be divided into three main categories: radially, tangentially and longitudinally dominant modes, consistent with expectations. Initial inspection of the ABAQUS contour plots quickly confirmed the previously identified radially dominant modes, examples of which are shown in Figures 2, 3 and 4. These were easily identified using the deformation scaling of the visualisation module, making the exaggerated mode shapes easier to observe and the coloured contours highlighting areas of greater deformation. The deformation scaling is arbitrary and automatically determined in ABAQUS in order that the mode shapes are readily interpretable. There are a number of colormaps available, of which “rainbow” – which is shown here – is the default. Red is the max deformation, irrespective of sign, while blue is zero deformation. Using the animation functionality enabled the longitudinal modes and tangential “twister” modes to be identified.

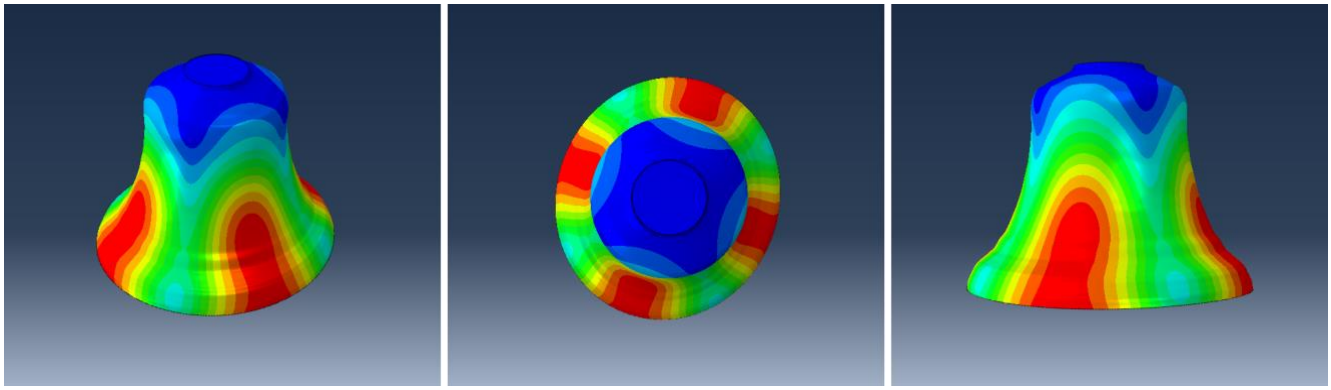

Figure 2 – Isometric, top and side view of "Hum" mode (2,0)

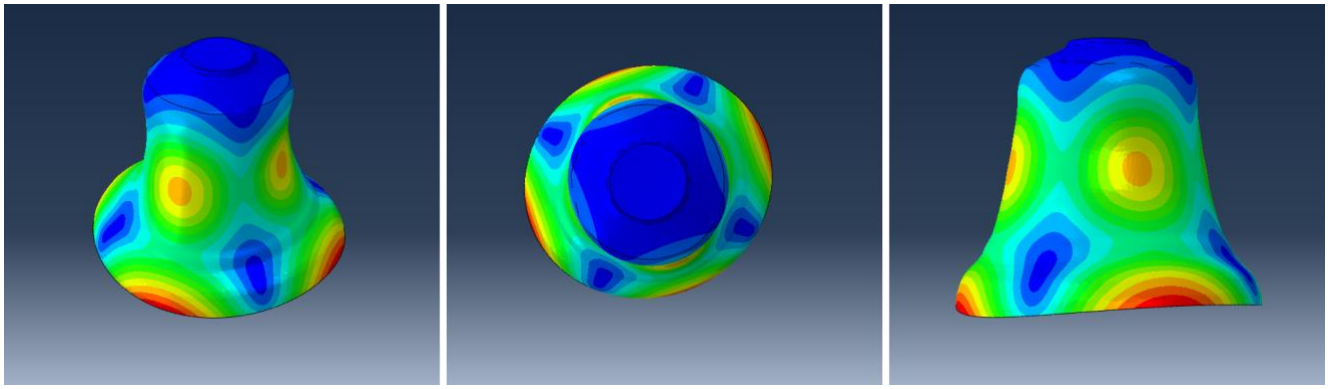

Figure 3 – Isometric, top and side view of "Fundamental" mode (2,1)

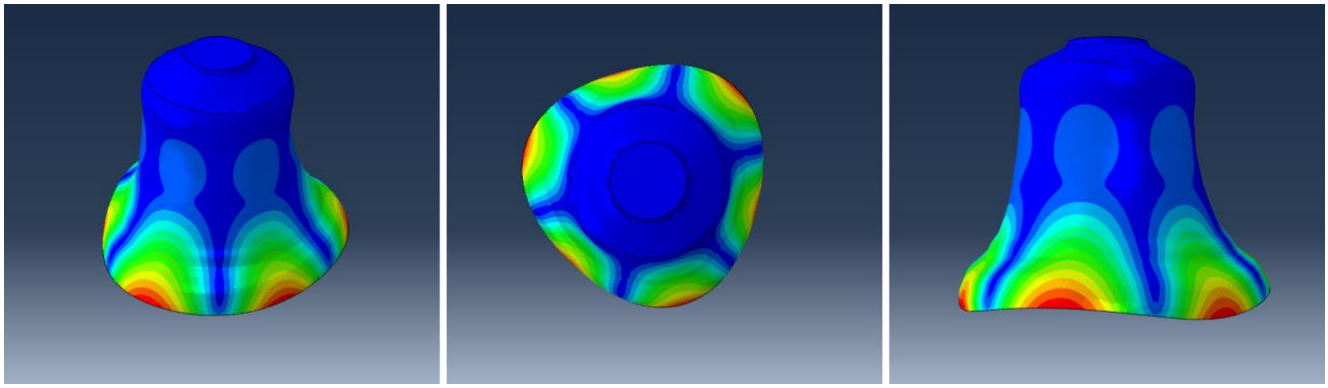

Figure 4 – Isometric, top and side view of "Tierce" mode (3,1)

By superimposing the scaled deformation vectors onto the mode shapes, it becomes possible to additionally identify the expected tangentially driven modes – previously observed but unidentified – with m values greater than 0. Figure 5 shows an example of a mode that was previously misclassified as radially or longitudinally dominated. With the deformation vectors superimposed, the mode was subsequently revealed to have large tangential components. Longitudinal modes, such as that shown in Figure 6, also became identifiable using this display option.

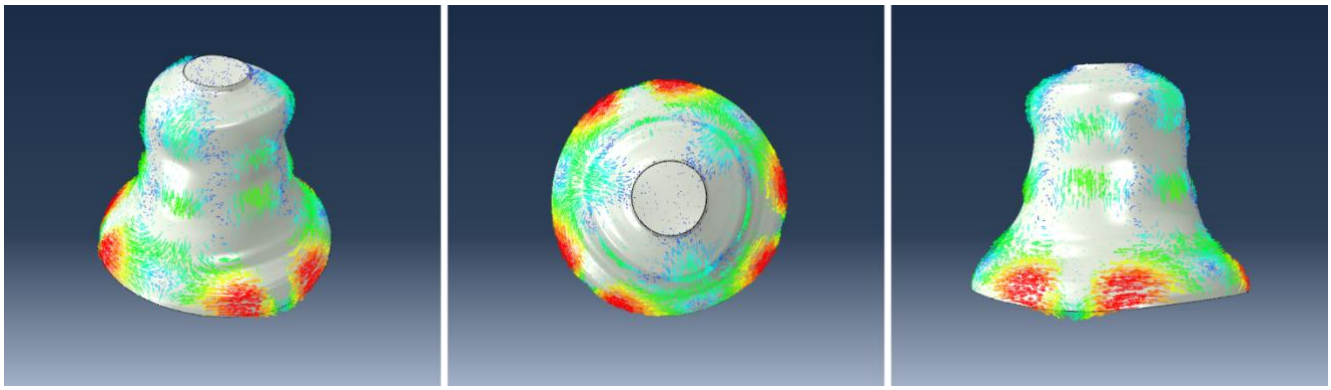

Figure 5 – Isometric, top and side view of tangential mode, 5462 Hz (3,4)

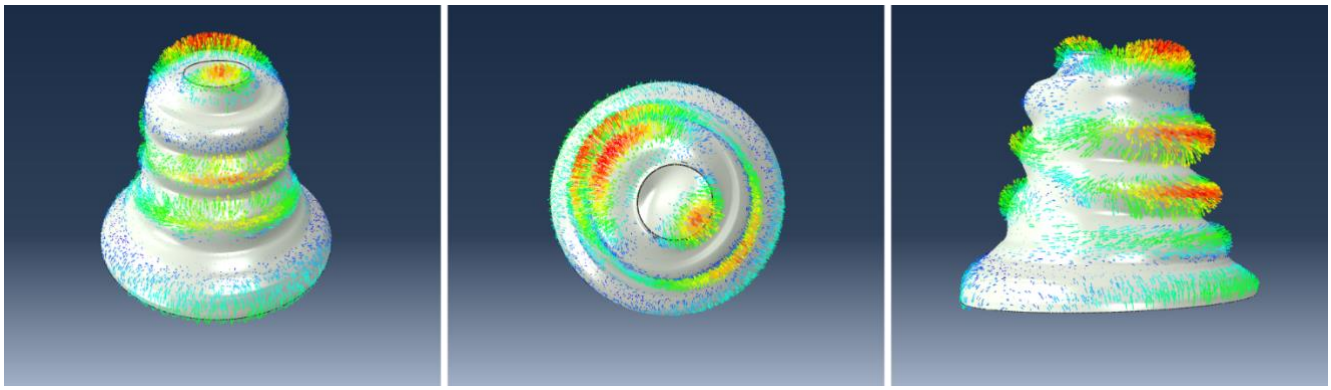

Figure 6 – Isometric, top and side view of m=1 longitudinal mode, 6842 Hz (1,7?)

3 MODE SHAPE DEFORMATION ANALYSIS

Processing of the ABAQUS results was performed to validate the classification and inspect for relationships between the radial, tangential and longitudinal components of deformation. Using a reduced mesh density for processing expediency, the nodal displacement field data for multiple examples of radial, longitudinal and tangentially driven modes were extracted from ABAQUS for post processing. The primary concern was the selection of node samples that were satisfactorily representative of the mode's overall deformations. Furthermore, conversion of the outputted X, Y and Z data into deformations in the radial, longitudinal and tangential directions, was necessary. Along with the calculations for processing the output data, three methods of node sampling were proposed and investigated which are: i) parallel (to the symmetry axis) cut, ii) normal (to the symmetry axis) cut and iii) whole bell.

3.1 Calculations

As the longitudinal direction is defined as that which is parallel to the axis of symmetry, i.e. the *y* axis in ABAQUS, the longitudinal displacement was accepted as directly output by ABAQUS. To calculate the radial and tangential displacements, however, the field output results from the *x-z* plane were converted using the following equations:

$$d_r = d_{x-z} \cdot u_r \tag{1a}$$

$$d_t = d_{x-z} \cdot u_t \tag{1b}$$

where d_r is the radial displacement, d_t is tangential displacement, $d_{x\text{-}z}$ is the field output displacement in the *x* and *z* directions and u_r/u_t are the unit vectors in the radial/tangential direction respectively. Using these expressions, the deformation of each node can be calculated in terms of cylindrical coordinates. The displacements of each mode were summarised by summing the absolute value of every node's radial, longitudinal and tangential displacements respectively to compare them.

3.2 Parallel or Normal Cut

The first Parallel Cut method of node selection considered was the taking of a section cut *parallel* to the symmetry axis, intersecting with the location of an antinode. Analysis was performed on the displacement field output of the nodes of elements that intersect with the section cut, as shown in Figure 7a for the Quint musical mode.

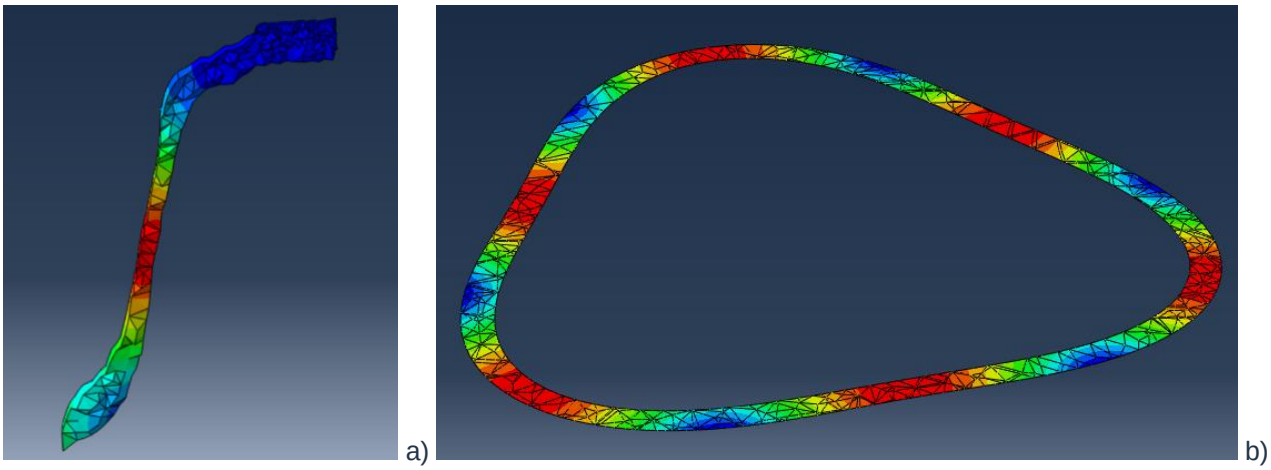

Figure 7 – a) Parallel element set and, b) Normal element set through antinode of 884 Hz 'Quint' (3,1) mode shape

The processing results of a selection of the three categories of deformation dominance shown in the Table 2 below. Of note, each examined mode showed consistency between the observed dominant deformations and calculated largest magnitude of displacement, as identified in Table 2 with **bold** typeface.

Table 2 – Parallel Cut Deformation Results using m nomenclature

Mode name or number (from Abaqus)	Dominant deformation (by inspection)	ABAQUS frequency (Hz)	m	Deformation		
				Radial	Longitudinal	Tangential
Fundamental	Radial	579.4	2	**73.7**	49.9	2.7
Quint	Radial	884.3	3	**81.6**	32.2	2.9
43/44	Longitudinal	2467.1	2	36.4	**66.8**	1.4
176/177	Longitudinal	6842.1	1	214.4	**244.0**	22.1
131/132	Tangential	5461.7	3	23.3	19.2	**58.0**
191/192	Tangential	7149.3	2	62.7	9.9	**147.4**

The Normal Cut method involved the taking of a section cut *normal* to the symmetry axis, intersecting with the antinode of the mode. Figure 7b again shows this approach for the Quint mode. For the many modes with deformation dominated at the rim, such an approach will omit a large proportion of deformation. This can be observed in Figure 8 for the case of the Fundamental. For this reason, this method is not included for subsequent analysis. Further investigation may, however, be warranted with cuts at other antinodes with different values of z.

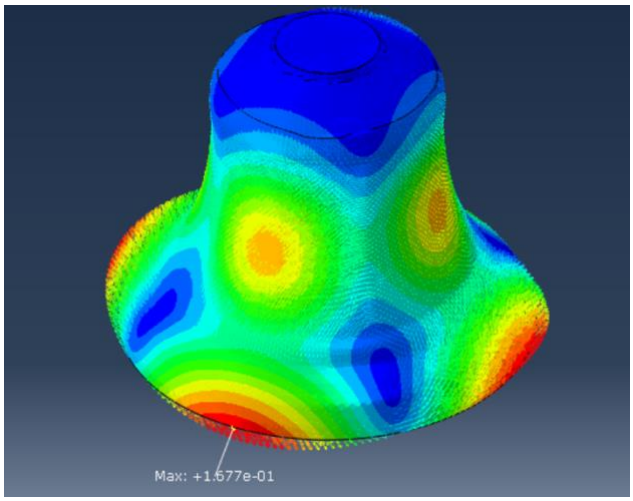

Figure 8 – The 579.5 Hz Fundamental (2,1); antinode indicated

3.3 Whole Bell

The final method utilised the entire bell model as the node sample for data collection. The results of the post processing of the whole bell are shown in Table 3 below. Similarly to the parallel cut method, the calculated displacements are consistent with the expected dominant deformation of each mode.

Table 3 – Whole Bell Deformation Results using m nomeclature

Mode name or number (from Abaqus)	Dominant deformation (by inspection)	ABAQUS frequency (Hz)	m	Deformation		
				Radial	Longitudinal	Tangential
Fundamental	Radial	579.4	2	**2231.6**	1977.2	1161.9
Quint	Radial	884.3	3	**2842.0**	1175.8	984.4
43/44	Longitudinal	2467.1	2	1719.5	**3344.8**	695.8
176/177	Longitudinal	6842.1	1	4786.1	**5202.4**	2390.6
131/132	Tangential	5461.7	3	1710.8	1689.0	**2711.9**
191/192	Tangential	7149.3	2	4211.7	1327.9	**4228.3**

3.4 Deformation Ratios

Due to the symmetry properties of any given mode in the axisymmetric bell, it becomes valuable to investigate the ratio between relevant deformations in the different cylindrical coordinate directions. For example, given a radially dominated mode of m > 0, the radial deformation can be expected to be larger than the tangential (Leissa, 1973). It is less well known what the corresponding relationships will be for tangentially and longitudinally dominated modes. This is therefore of interest to explore using the techniques defined herein. Table 4 below provide a comparison of the ratios between relevant displacement components for the methods described above.

Table 4 - Expected vs. Observed Deformation Ratios (R=Radial, T=Tangential, L=Longitudinal)

Mode name or number (from Abaqus)	Dominant deformation (by inspection)	ABAQUS frequency (Hz)	m	Relevant ratio	Observed ratio	
					Parallel cut	Whole bell
Fundamental	Radial	579.4	2	R:T	24.7:1	**1.9:1**
Quint	Radial	884.3	3	R:T	27.3:1	**2.9:1**
43/44	Longitudinal	2467.1	2	L:R	1.8:1	**1.9:1**
176/177	Longitudinal	6842.1	1	L:R	1.1:1	**1.1:1**
131/132	Tangential	5461.7	3	T:R	2.5:1	1.6:1
191/192	Tangential	7149.3	2	T:R	2.3:1	1.0:1

It is interesting to note that, by inspecting the node sample through a parallel cut, the radial modes, and to a lesser extent the tangential modes, exhibit a notable exaggeration of the dominant deformation component when compared with the value of m. This indicates that the parallel cut approach is not fairly representing the deformation of the mode, perhaps because the high displacement areas are disproportionally overrepresented in the cuts. Meanwhile, the analyses of the longitudinal modes perform for the parallel cut show ratios that are in alignment with the value of m.

Meanwhile, the ratios obtained from analysis of the whole bell demonstrate ratios in close agreement with m for the radially and longitudinally dominated modes, as identified in Table 4 with **bold** typeface. This is an interesting finding, presented here for the first time, warranting further investigation. In the case of the tangentially dominated modes, it is currently unclear what drives the ratio of tangential to radial deformation.

4 CONCLUSIONS

The use of ABAQUS has allowed a new approach to the classification of modes of the English church bell. Enhanced visualisation including the superposition of deformation vectors onto the displayed mode shape and novel post-processing has allowed a more definitive classification of radially, longitudinally and tangentially dominated modes. Three options for extracting mode shape deformations were considered: a parallel cut, a normal cut and the whole bell. Ratios between the radial, tangential and longitudinal coordinates were in closer agreement with predictions – which are based on values of m – for all the modes considered with the whole bell

option. The ratios show some interesting trends, for radially and longitudinally dominated modes, but remain in need of further investigation, especially for tangentially dominated modes. The method robustness continues to be the topic of this research and its application to other axisymmetric structures is the topic of future investigation. Furthermore, future investigations will look to export ABAQUS parameters in cylindrical polar coordinates directly.

REFERENCES

Charnley, T., & Perrin, R. (1975). Torsional vibrations of bells. *Journal of Sound and Vibration*, 40(2), 227–231. https://doi.org/10.1016/s0022-460x(75)80243-4

Leissa, A. W. (1973). Vibration of Shells. *Ntrs.nasa.gov*. https://ntrs.nasa.gov/citations/19730018197

Perrin, R., & Charnley, T. (1973). Group theory and the bell. *Journal of Sound and Vibration*, 31(4), 411–418. https://doi.org/10.1016/s0022-460x(73)80257-3

Perrin, R., Charnley, T., & dePont, J. (1983). Normal modes of the modern English church bell. *Journal of Sound and Vibration*, 90(1), 29–49. https://doi.org/10.1016/0022-460x(83)90401-7

Perrin, R., Elford, D., Chalmers, L., Swallowe, G. M., Moore, T. R., Hamdan, S., & Halkon, B. J. (2014). Normal modes of a small gamelan gong. *Journal of the Acoustical Society of America*, 136(4), 1942–1950. https://doi.org/10.1121/1.4895683

Perrin, R., Swallowe, G. M., Zietlow, S. A., & Moore, T. R. (2008). The Normal Modes of Cymbals. *Proc. Inst. Acoustics*, 30, 460–467.

Rossing, T. D. (1984). The Acoustics of Bells: Studying the vibrations of large and small bells helps us understand the sounds of one of the world's oldest musical instruments. *American Scientist*, 72(5), 440–447. http://www.jstor.org/stable/27852858

Rossing, T. D., & Perrin, R. (1987). Vibrations of bells. *Applied Acoustics*, 20(1), 41–70. https://doi.org/10.1016/0003-682x(87)90082-x

Wolbarst, A.B. (1977). Symmetry and Quantum Systems. Van Nostrand Reinhold Company, New York.